Heterogeneous genomic architecture of skeletal armour traits in sticklebacks

Abstract

Whether populations adapt to similar selection pressures using the same underlying genetic variants depends on population history and the distribution of standing genetic variation at the metapopulation level. Studies of sticklebacks provide a case in point: when colonising and adapting to freshwater habitats, three-spined sticklebacks (*Gasterosteus aculeatus*; TSSs) with high gene flow tend to fix the same adaptive alleles in the same major loci, whereas nine-spined sticklebacks (*Pungitius pungitius*; NPSs) with limited gene flow tend to utilize a more heterogeneous set of loci. In accordance with this, we report results of quantitative trait locus (QTL) analyses using a F_2 back-cross design showing that lateral plate number variation in the western European lineage of NPSs mapped to three moderate-effect QTL, contrary to one major QTL in TSSs and these QTL were different from the four previously identified QTL in the eastern European lineage of NPSs. Furthermore, several QTL were identified associated with variation in lateral plate size, and three moderate-effect QTL with body size. Together, these findings indicate that genetic underpinnings of skeletal armour variation in *Pungitius* sticklebacks are more polygenic and heterogenous than those in three-spined sticklebacks, indicating limited genetic parallelism underlying armour trait evolution in the family Gasterostidae.

Key words: body size, lateral plate, parallel evolution, *Pungitius pungitius*, QTL

Introduction

Why and when evolution can be repeatable and predictable remains a longstanding question in biology. Parallel evolution has been the prevailing hypothesis explaining repeatable phenotypic evolution (Martin and Orgogozo, 2013) by a set of identical-by-descent genetic variants controlling

the same adaptive traits in multiple independent evolutionary lineages (Schluter et al. 2004). The probability of parallel evolution depends on many factors (MacPherson and Nuismer 2017; Bolnick et al. 2018), including how standing genetic variation is distributed at the metapopulation level (Fang. et al. 2020; Fang et al. 2021; Kemppainen et al. 2021; Schlötterer 2023). When populations are well connected, adaptive alleles are easily transported from one population to another and thereby available to be picked by selection in multiple populations subject to similar environmental pressures (Ralph and Coop 2015; Bailey et al. 2017; Lee and Coop 2017; Roberts-Kingman et al. 2021). However, once gene flow is sufficiently restricted, the potentially adaptive alleles may not reach all populations, forcing selection to work with alternative alleles in different loci (Merilä 2014; Kemppainen et al. 2021). The likelihood of parallel evolution is also influenced by demographic history of populations (MacPherson and Nuismer 2017; Thompson et al. 2019): parallel evolution is less likely in small populations where bottlenecks and strong genetic drift result in the stochastic loss of adaptive alleles (Leinonen et al. 2012; Fang et al. 2020; Dahms et al. 2022). Accordingly, smaller and less connected populations tend to have more heterogeneous genetic architectures underlying the same morphological transitions even if driven by similar ecological pressures, resulting in non-parallel evolutionary responses to selection. Understanding the relative contributions of parallel and non-parallel genetic changes to repeated phenotypic evolution in the wild can improve theoretical understanding of the role of natural selection in shaping genetic variation (Johanneson 2001) and inform predictions on the evolutionary potential of species and populations to cope with ongoing environmental changes (Bay et al. 2017).

While early research found ample evidence of genetic parallelism at both species and population levels (Colosimo et al. 2005; Stewart and Thompson 2009; Bernatchez et al. 2010; Elmer et al. 2010), it is now becoming increasingly clear that parallelism is perhaps not as common as previously thought (e.g., Bolnick et al. 2018; Fang et al. 2020; Kemppainen et al. 2021; Schlötterer 2023). The prevailing hypothesis of parallel evolution could thus stem from an ascertainment bias driven by the novelty value of discovering evidence for genetic parallelism, as well as from focus

on systems characterized by high genetic connectivity. On the other hand, non-parallelism is more likely to dominate in species characterized by low genetic connectivity and small effective population sizes. The stickleback fishes have been popular model systems to study the repeatability of evolution during their numerous and recurrent colonisations from marine to freshwater habitats throughout past glacial cycles (e.g., Colosimo et al. 2005; Coyle et al. 2007; Marchinko and Schluter, 2007; Chan et al. 2010; DeFaveri et al. 2011, 2013; Jones et al. 2012; Merilä 2013; Fang et al. 2021; Kemppainen et al. 2021; Reid et al. 2021; Roberts-Kingman et al., 2021). What has transpired from these studies is that in the case of the three-spined stickleback (*Gasterosteus aculeatus*), adaptation to the freshwater environment is typically achieved by parallel genetic changes in major-effect loci (Colosimo et al. 2005; Chan et al. 2010; Peichel and Marques, 2017; Reid et al. 2021; but see: DeFaveri et al. 2011; Leinonen et al. 2012; Erickson et al. 2016; Fang et al. 2021). However, in the case of the nine-spined stickleback (*Pungitius pungitius*), there is much less genetic parallelism over similar geographic distances in response to adaptation to freshwater environments (Shikano et al. 2013; Fang et al. 2021; Kemppainen et al. 2021). For example, pelvic reduction is underlied by one major-effect locus in different freshwater populations of three-spined sticklebacks (Chan et al. 2010), whereas in the case of nine-spined sticklebacks it is underlied by a range of genetic architectures from single locus to polygenic systems (Kemppainen et al. 2021).

Another textbook example of predictable and repeatable evolution is the lateral plate number reduction in freshwater three-spined sticklebacks after colonization from marine habitats (Colosimo et al. 2005). The majority of their freshwater populations worldwide have achieved lateral plate reduction via inheritance of the same ancestral allele associated with the Ectodysplasin-A gene (*Eda*; Colosimo et al., 2005; O'Brown et al. 2015). Quantitative trait locus (QTL) mapping studies have revealed that the QTL containing *Eda* gene explains 69% - 98% variation in lateral plate phenotypes (Colosimo et al. 2004; Liu et al. 2014; Glazer et al. 2015; Erickson et al. 2016; Schluter et al. 2021; see also: Loehr et al. 2012), suggesting large-effect single-locus basis for this ecologically important adaptive trait. However, the *Eda* gene was not associated with lateral plate

variation in nine-spined sticklebacks from North America (Shapiro et al. 2009) or eastern Europe (Yang et al. 2016). Instead, Yang et al. (2016) mapped the genetic architecture of lateral plate variation in the eastern European lineage (EL) of nine-spined sticklebacks to four different chromosomes (linkage groups LG8, LG12, LG20, LG21), none of which included the *Eda* gene. These studies thus suggest major interspecific differences in genetic architectures of lateral plate variation within the stickleback family Gasterosteidae, as well as a more polygenic and heterogeneous genetic architecture for this trait in the genus *Pungitius*.

The main aim of this study was to address the repeatable phenotypic evolution hypothesis (Martin and Orgogozo, 2013) in the context of genetic architectures of lateral plate phenotypes in *Pungitius* sticklebacks. To test the hypothesis of parallel evolution, we mapped QTL associated with variation in lateral plate numbers utilizing a F_2-generation backcross family between two closely related *Pungitius* species: the fully plated *P. sinensis* and the partially plated *P. pungitius* from the western European lineage (WL). The WL *P. pungitius* has a distinct evolutionary history from the eastern European lineage (EL; Teacher et al. 2011; Guo et al. 2019; Feng et al. 2022) and has not yet been studied regarding their armour plate genetic architecture. The repeatable evolution hypothesis predicts that lateral plate number variation in the WL should be controlled by allelic variation either in the same genetic locus as that in the sister species three-spined stickleback or the previously identified QTL in the EL *P. pungitius*. The alternative hypothesis of non-parallel evolution of the same morphology underlied by different QTL is also plausible in the light of previous QTL analyses of lateral plate number variation in *Pungitius* sticklebacks (Shapiro et al. 2009; Yang et al. 2016). The secondary aims of this study were to identify QTL associated with lateral plate size and body size variation in *P. pungitius*, as well as capitalize the opportunity to narrow down the location of the sex determination region in *P. sinensis* (cf. Natri et al. 2019) with the aid of a dense set of SNPs and an improved *Pungitius* reference genome (Kivikoski et al. 2021).

Material and Methods

Crosses and fish rearing

A fully plated female *P. sinensis* from Yoneshiro River, Odate, Japan (40°16' N, 140°29' E) was artificially crossed with a partially plated male *P. pungitius* from Brugse polders, Maldegem, Belgium (51°10' N, 03°28' E) and the resulting F_1 hybrids were reared in a 28-l tank at 16 °C until mature. The F_1 hybrid males of these crosses were found to be sterile (Natri et al. 2019), and thus a backcross was conducted by naturally mating a partially plated F_1 hybrid female with an outbred fully plated *P. sinensis* male (Fig. 1). This backcross mating was carried out in a 6-l tank with a zebrafish rack system (Aquaneering Inc., USA) to obtain fertilized clutches repeatedly. From three days post-hatching, larvae were fed twice daily with newly hatched brine shrimp (*Artemia sp.*) nauplii. Approximately eight weeks post-hatching, frozen bloodworms (Chironomidae larvae) were added to their diet. The 24-h photoperiod was maintained during the rearing. Wild fish were obtained in accordance with national and institutional ethical regulations with permission from the Finnish Food Safety Authority (#1181/0527/2011 and #3701/0460/2011). All fish rearing was conducted under the license from the Finnish National Animal Experiment Board (#STH379A and #PH1236A).

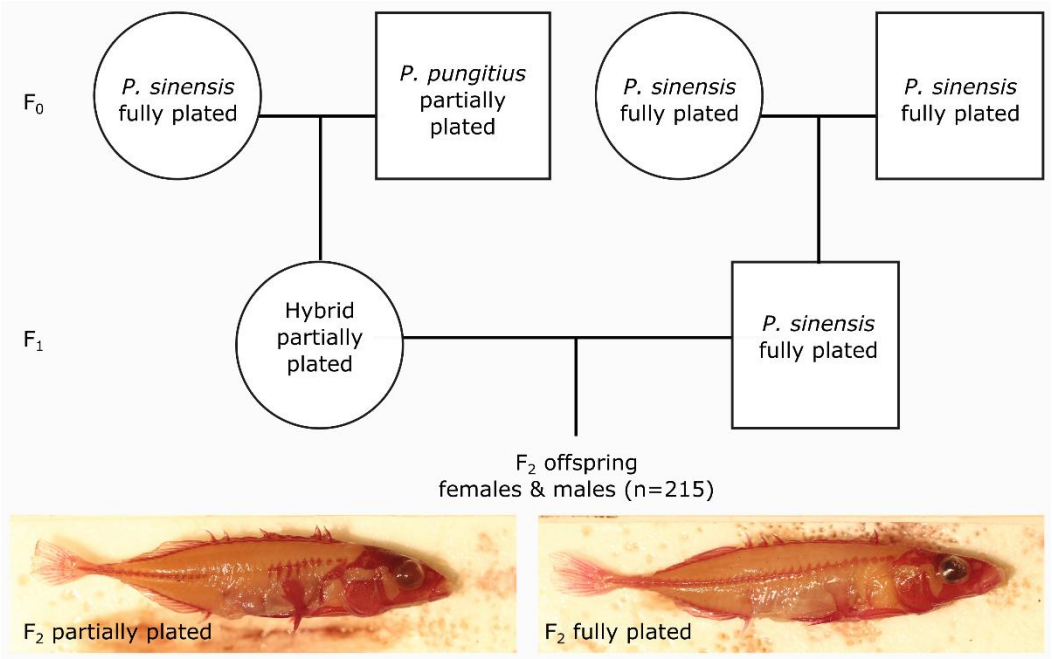

119

120 **Figure 1. The backcross experiment between fully plated *Pungitius sinensis* from Japan and**
121 **partially plated *P. pungitius* from Belgium.** Circles represent females and squares represent
122 males. The two photos show fully plated and partially plated phenotypes of the F_2 progeny stained
123 with alizarin red.

124

125 The F_2 progeny were reared in 28-l tanks (20–30 fish per tank) at 16°C for 40 weeks after hatching.
126 At the end of the experiments, the wild-caught grandparents (F_0), F_1 parents, and F_2 offspring were
127 euthanized with MS-222 (Tricaine methanesulfonate) and stored in ethanol. A fin clip was taken
128 from all individuals and preserved at -18°C for DNA extractions. In total, 215 F_2 offspring from six
129 clutches were available for the analyses (Table S1). Phenotypic measurements (see below) were
130 taken from these F_2 offspring and their sex was recorded based on gonadal inspection after
131 dissection.

132 *Phenotypic measurements*

133 Firstly, the ethanol-stored carcasses of F_2 offspring were fixed in 4% formalin and stained with
134 alizarin red following the standard procedure (e.g., Trokovic et al. 2011) to visualize bony

135 structures. Subsequently, phenotypes were quantified by ImageJ
136 (https://imagej.nih.gov/ij/index.html) from photographs (Fig. 1; Fig. S1) of the stained fish.
137 Standard length and maximum body height of each specimen was measured to nearest 0.01mm
138 from the photographs.

139 Plate and myomere numbers were counted on both sides of the body under a dissecting microscope.
140 The proportion of plated myomeres on each side was calculated to represent the level of platedness.
141 The height, width and surface area of the largest lateral plates were measured on both sides of the
142 body. Most of the largest plates were found on myomere seven counted from the anterior part of the
143 body towards the tail (Fig. S1). If the fish had no plate in these positions, the largest plate located
144 within the first 15 anterior myomeres were measured instead with their myomere position recorded.
145 We did not measure plates on the myomere positions > 15 because plates in the posterior region
146 have distinct shapes and sizes compared to those in more anterior positions. Measurements of the
147 same phenotype on the left and right sides of the body were highly correlated ($r > 0.86$, $p < 1e\text{-}10$;
148 Fig. S2). Therefore, in the following analyses we used average values of each measurement of the
149 two sides.

150 The distribution of phenotypic measurements was visualized in R (R core team 2022). Traits fitting
151 the normal distribution (namely standard length, body height, plate area, plate height, and plate
152 width; Fig. S3) were analysed using raw values. Distributions of the plate number and the
153 proportion of plated myomeres were left-skewed and bimodal because of the presence of only fully-
154 and partially-plated individuals (Fig. S3). This pattern is related to our experimental design (Fig. 1)
155 where offspring genotypes can only be *P. sinensis* homozygotes (SS, likely fully-plated) or *P.*
156 *sinenesis*-*P. pungitius* heterozygotes (SP, likely partially-plated). Therefore, the missing *P.*
157 *pungitius* homozygous genotypes likely account for the lack of low-plated individuals (WL *P.*
158 *pungitus* have on average 5.4 lateral plates; Banarescu and Paepke 2001) and the left skew of plate
159 number distribution. We first conducted QTL analyses on the mean number of plates
160 (plateN_mean) as a numeric trait. To account for the lack of normality in the distribution of raw

data, we also conducted QTL analyses on two transformed binary traits. First, the plate number was transformed into a binary trait, plateN_binary, where individuals were labeled as partially-plated if having the mean number of plates ≤ 25 (around the peak of the first phenotype cluster, Fig. S3) and the rest of the individuals were fully-plated. Second, the proportion of plated myomeres was transformed into the binary trait, plateness, where individuals having 100% plated myomeres on both sides were considered fully-plated while the rest were partially-plated.

Sequencing and genotyping

DNA was extracted from the preserved fin-clips of wild-caught grandparents, F_1 hybrid parents, and F_2 offspring using the modified salting out method of Sunnucks and Hales (1996). Libraries for the restriction-site associated DNA sequencing (RADseq) were prepared using the *PstI* restriction enzyme (Miller et al. 2007). The prepared libraries were sequenced on an Illumina HiSeqTM 2000 (BGI Hong Kong). Demultiplexed raw sequencing data were obtained from BGI with adapter and low-quality reads removed. These reads were around 43bp in length and they were mapped to the reference genome of *Pungitius pungitius* (version 7, Kivikoski et al. 2021) using the BWA v0.7.17 backtrack algorithm (bwa aln and bwa samse; Li and Durbin 2009). The mapped reads were reformatted, sorted, and indexed using SAMtools version 1.16.1 (Danecek et al. 2021). Genotyping was conducted according to the sequencing data processing pipeline of Lep-MAP3 (Rastas 2017). Briefly, SAMtools mpileup (Li 2011) was run on the mapped data by linkage group. The version 7 reference genome has 21 linkage groups (LGs) and 1645 unassembled contigs (including a mitochondrial genome). Very few data were mapped to the unassembled contigs whose physical positions were unclear. Therefore, we only used the data mapped to the 21 linkage groups as the input of the Lep-MAP3 module Pileup2Likelihoods to estimate genotypes.

Linkage map construction

Linkage maps were constructed following the Lep-MAP3 default pipeline (Rastas 2017). Briefly, the module ParentCall2 was run on all genotyped individuals (offspring, parents, grandparents) with

the noninformative sites removed (removeNonInformative=1). The retained genotypes were processed by the module Filtering2 with the parameter dataTolerance=0.001 (i.e., segregation distortion limit 1:1000). Then the module SeparateChromosomes2 was run to assign markers to linkage groups (ordered by size) using the parameter lodLimit=50. The first (i.e., largest) 21 linkage groups were retained, corresponding to the number of chromosomes in the reference genome (Fig. S4). The linkage map was modified by collapsing all the other linkage groups with unassigned singletons. Next, the module JoinSingles2All was run using the modified linkage map and the non-filtered genotyping data (the output from ParentCall2) to map as many singletons to the 21 linkage groups as possible, using the parameters lodLimit=40, lodDifference=2, lod3, Mode=3, iterate=1, and distortionLod=1. Finally, the module OrderMarkers2 was used to order markers in the mapped 21 linkage groups and generate phased maternal maps using commands outputPhasedData=1 and informativeMask=2.

To get optimal results, OrderMarkers2 was run five times independently for each linkage group and the runs having the highest likelihoods were used as the optimal parent-phased maps. These optimal maps were then evaluated in OrderMarkers2 (command evaluateOrder) with additional parameters improveOrder=0 and grandparentPhase=1 to convert them into grandparental phases. The optimal parental phases and corresponding grandparental phases were matched using the phasematch.awk script of Lep-MAP3. The matched maps were converted back to genomic coordinates using the awk script in Lep-MAP3, and the maps were re-named by chromosomes based on the physical positions of their markers. In each map, the few markers that were located in different physical chromosomes were removed. Then the converted linkage maps were visualized by plotting the genetic position (centiMorgan, cM) against the physical position (bp), and the maps were further cleaned by manually removing the outlier markers and markers that generated gaps at the start or end of each linkage map. Finally, the map2genotypes.awk script of Lep-MAP3 was used to convert the cleaned maps into F_2 genotypes.

QTL mapping

The QTL mapping was conducted using the software R/qtl2 (Broman et al. 2019). The genotypes and linkage maps obtained from Lep-MAP3 were reformatted for R/qtl2 using custom scripts. Backcross (bc) cross type was specified in the control files. Pseudomarkers were inserted into genetic maps at the distance of 1 cM. Genotype probabilities were calculated using the error probability of 0.002. Genotype-phenotype associations were estimated by conducting genome scans (command scan1) using the default simple linear method of the Haley-Knott regression. The other R/qtl2 parameters were kept as default unless stated otherwise. Statistical significance thresholds were established using 1000 permutations (command scan1perm). The obtained significant threshold (p=0.05) was used to identify QTL peaks and their 95% Bayes credible intervals (CI) using the command find_peaks (peakdrop=2).

We first conducted QTL mapping on the binary phenotypic sex. Pearson's Chi-squared test showed that phenotypic sex was not dependent on the clutch identity ($p = 0.798$) and thus we did not add any covariate in this model. The model was run on all 215 F_2 offspring, including 109 phenotypic females, 105 phenotypic males, and one individual of unknown phenotypic sex. Preliminary analyses indicated misidentified phenotypic sex in 11 individuals (see supplementary information) which were removed together with the sex-unknown individual from downstream analyses for clarity.

QTL mapping on the body size measurements (standard length and body height) was carried out with sex and clutch included as additive covariates (argument addcovar) because both phenotypes showed significant dependency on sex and clutch in tests of the Analysis of Variance (ANOVA; Table S2). For the binary traits, plateN_binary and plateness, we tested their dependency on sex and clutch identities using the Pearson's Chi-squared test and their dependency on the standard length and body height using t-tests. None of the variables showed significant relationships ($p > 0.05$) with either binary traits. Therefore, no covariate was added in the QTL mapping of plateN_binary or plateness. For each of the other numeric traits (plate number, plate area, plate height, plate width), the dependency on sex and clutch was first tested using ANOVA. Then a generalized linear model

of each trait was fitted on the detected significant independent variables, and the residuals were used to further test dependency on standard length and body height (i.e., with sex and clutch controlled; Miller et al. 2014). All significant independent variables were then included as additive covariates in the QTL mapping of the corresponding trait (Table S2).

The genomic regions spanning the 95% CIs around significant QTL were considered as QTL regions. The percentage of phenotypic variation explained (PVE) by each significant QTL peak was calculated as $PVE = 1 - 10^{-\frac{2}{n}*LOD}$ where *n* is the sample size and LOD is the logarithm of the odds of the QTL peak (Broman and Sen 2009; Smith et al. 2020). In addition, for each trait, we also used a previously described lasso regression approach to jointly incorporate all SNPs into a multilocus model to estimate the total PVE value that approximates the narrow sense heritability of a given trait (Li et al. 2017, 2018; Kemppainen et al. 2021). To facilitate calculation of the lasso algorithm, the same genotype file as used for R/qtl2 analyses was re-coded by removing duplicate SNPs that had the same genotypes (2 677 SNPs retained) and merging all SNPs outside significant QTL regions into one chromosome representing the non-QTL region. For each trait (excluding sex), the total PVE was estimated using all remaining SNPs, and the PVE of each QTL was estimated using the SNPs corresponding to the given QTL region. All phenotypic analyses and QTL mapping were conducted using R version 4 (R Core Team 2022).

QTL effects and candidate genes

As we were mostly interested in traits related to lateral plate variation (i.e., plate number and plate size), we further estimated the effects of all the combinations of identified QTL peaks in these traits. QTL effects were estimated using the command scan1coef and plotted using plot_coef in R/qtl2. The most likely genotypes of the analyzed F_2 offspring at each QTL peak were extracted using the command maxmarg in R/qtl2. Phenotypes were plotted against genotypes at each QTL peak position and by combinations of all identified QTL peaks.

For each QTL region, we extracted all physical markers which mapped to genetic positions within these regions and identified all genes containing these physical markers. Gene lists were made using the annotation of the version 6 reference genome (Varadharajan et al. 2019) and liftover between version 6 and version 7 reference genomes (Rastas 2020; https://sourceforge.net/p/lep-anchor/code/ci/master/tree/liftover.awk).

Results

Genotyping and linkage maps

The final dataset consisted of 221 individuals which included four F_0 grandparents, two F_1 parents, and 215 F_2 offspring (Fig. 1). The Lep-MAP3 Pileup2Likelihoods module identified 170 339 SNPs across the 21 linkage groups of which 84 526 informative sites were retained by ParentCall2. The largest 21 LGs identified by SeparateChromosomes2 contained 61 863 markers (Fig. S4) and the remaining 22 663 sites were designated as singletons. Finally, JoinSingles2All further added 7 485 sites into the linkage groups, resulting in a total of 69 348 sites separated into 21 LGs. Preliminary results showed that fewer than 8% of markers were paternally informative (i.e., using informativeMask=13) while more than 92% of the markers were maternally informative (informativeMask=23). This observation may not be surprising given that only the F_1 mother was hybrid and that the males in general have fewer crossovers (Kivikoski et al. 2023). In addition, the *P. pungitius* reference genome was used which was more similar to the hybrid F_1 female than the F_1 male (*P. sinensis*). Therefore, only the maternally informative markers were utilized in the following analyses. The phased and matched maternal maps had a total of 60 089 sites, and 59 629 sites were retained after the manual cleaning (Fig. S5).

QTL mapping of sex

The previous study by Natri et al. (2019) found that sex of hybrids between *P. sinensis* (ZW system) and *P. pungitius* (XY system in most lineages, unknown in WL) was controlled by the ZW system inherited from *P. sinensis* and mapped to a 19.4 cM region on LG12. In agreement with this, we found a strong association between phenotypic sex and LG12 and we narrowed down the sex determination region to two nearby QTL (in total 1 cM) with non-overlapping 95% CIs (Table 1). All F_2 males were homozygous and F_2 females heterozygous at the highest QTL peak at 11.826 cM except for 11 individuals (Fig. S6, S7) which were removed together with the individual of unknown sex (Table S1), retaining 203 individuals for the downstream analyses. The two QTL regions contained 43 SNPs located within six genes (*Usp7*, *EFS*, *DHRS4*, *Slc7a8*, *Svep1* and *TBC1D19*; Table S3).

QTL mapping of lateral plate phenotypes

Most of the lateral plate phenotypes were significantly dependent on phenotypic sex (Table S2). Females had more (x = 30.1 ± 0.45 [S.E.]) and bigger (x = 2.0 ± 0.10 mm^2) lateral plates than males (plate number x = 28.7 ± 0.52, plate area: x = 1.6 ± 0.08 mm^2). However, this sexual dimorphism is confounded by body size (females are larger, see below), as *t*-tests of plate number and plate size between sexes were not significant ($p > 0.05$) after controlling for standard length. Both plate number and the percentage of plated myomeres (*viz*. plateN_mean, plateness) were associated with a QTL at almost the same peak position in LG13 with overlapping confidence intervals (Table 1; Fig. 2A). In addition, plate number was associated with QTL on LG17 and LG4 (Fig. 2A), the latter containing the candidate gene *Eda* that controls lateral plate phenotypes in three-spined sticklebacks (Colosimo et al. 2004). Almost identical QTL regions were found when using the raw values of the plate number (plateN_mean; Table 1) and the transformed binary trait (plateN_binary; Table S4; Fig. S8), providing confidence of the identified regions being true QTL rather than false positives despite a skewed distribution of raw plate numbers. Both the LG4 and the LG13 QTL showed a positive effect of the *P. sinensis* - *P. pungitius* hybrid genotype (SP) whereas the LG17 QTL showed a negative effect of the SP genotype on lateral plate numbers (Fig. 3A). Consistently,

among the eight genotype combinations of these three QTL, the genotype having SS at both LG4 and LG13 but SP at LG17 generated the lowest number of lateral plates, while the reverse (SP at LG4 and LG13 while SS at LG17) generated the highest number of lateral plates (Fig. 3B).

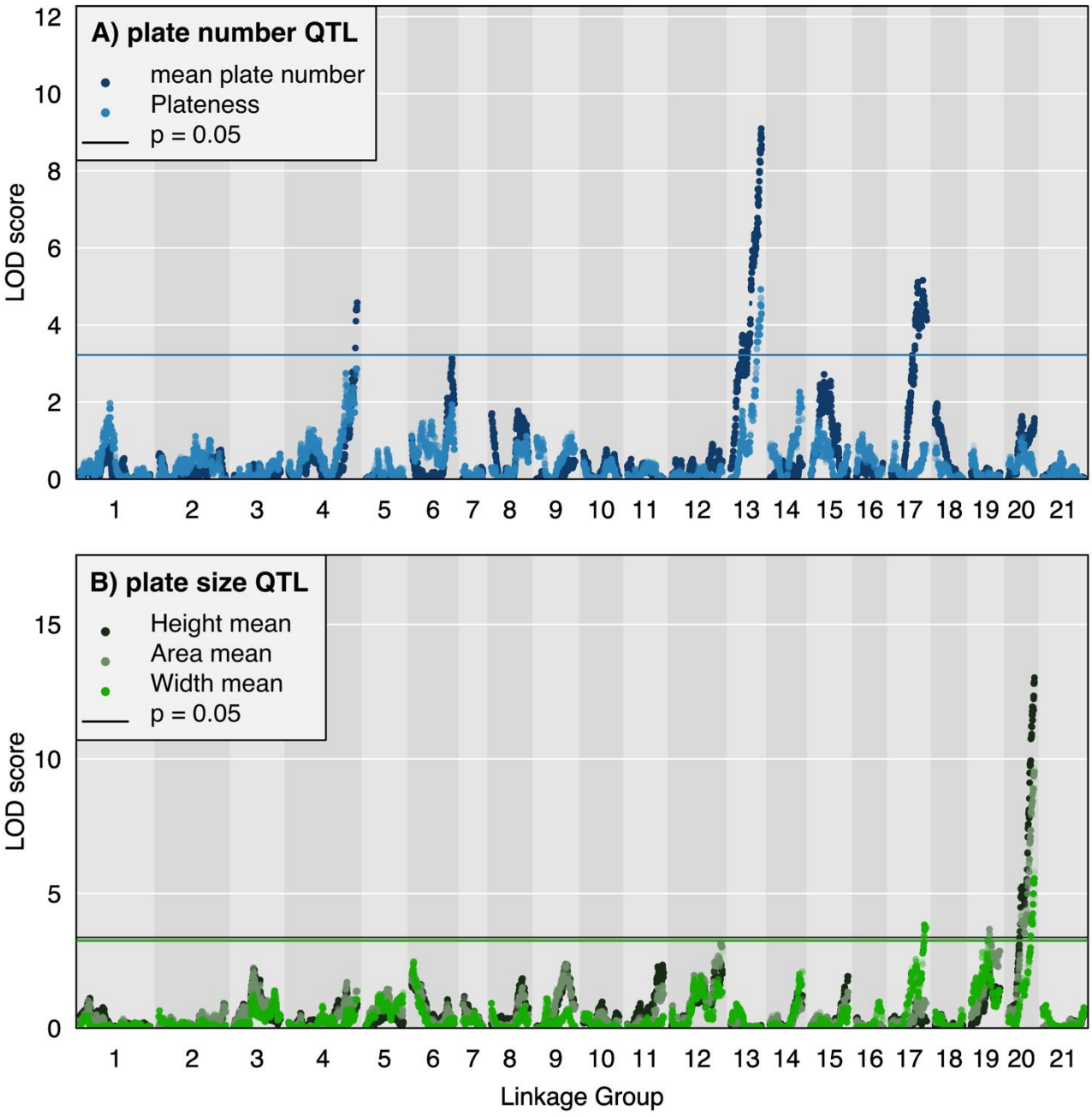

Figure 2. The QTL for lateral plate A) number and B) size in nine-spined sticklebacks. Horizontal lines show the significance threshold (p = 0.05) derived from 1000 permutation tests for each trait.

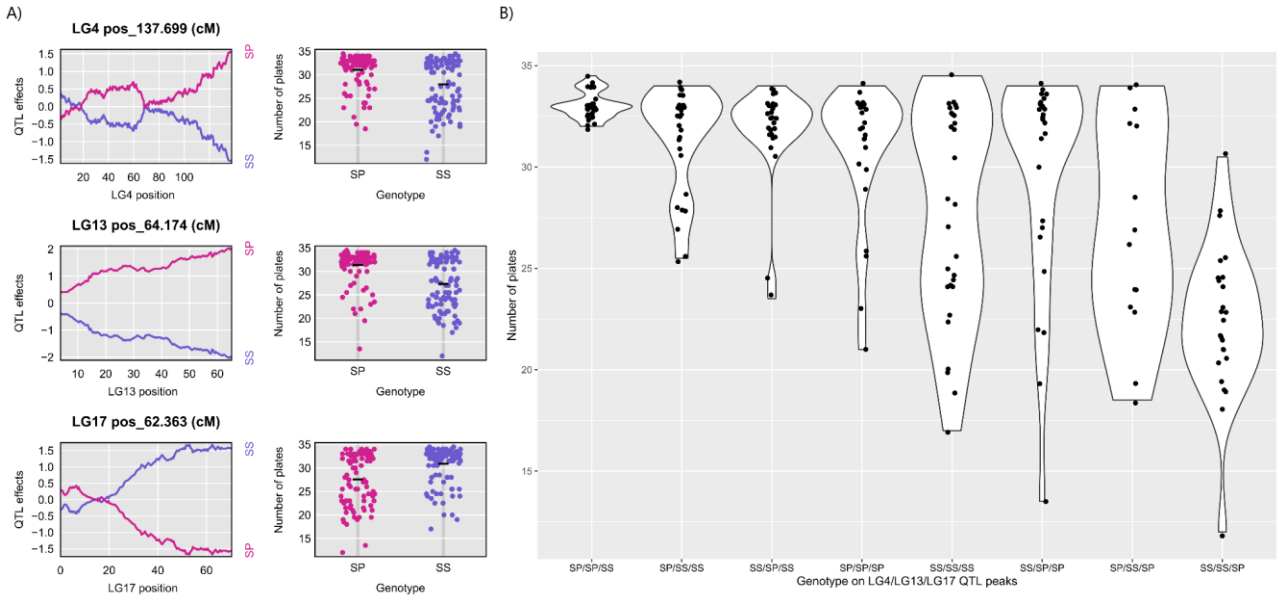

Figure 3. Effects of the genotypes at QTL peaks on lateral plate numbers. S represents the paternal allele from *P. sinensis* and P represents the maternal allele from *P. pungitius*. **A)** Effect size and phenotype-genotype plots of each QTL estimated by R/qtl2. **B)** Distribution of individual number of plates by genotype combinations at the three QTL.

The lasso regression approach produced a genomic estimate of heritability (h^2) at 0.486 (Table S5), a value higher than the summed PVEs of the three plate number QTL (Sum_{PVE} = 0.396; Table 1), indicating that there might be additional QTL influencing plate number, albeit their contributions are likely to be minor.

The plate size phenotypes (*viz*. area, height, and width of the largest plate) were all associated with the same QTL peak on LG20 (Table 1; Fig. 2B). Plate area and plate width also mapped to nearby QTL peaks on LG19, but their 95% CIs were almost as wide as the entire LG including large regions of LOD scores below the significance threshold (Fig. S9). In addition, plate width also mapped to LG17, overlapping with the QTL for plate number (Table 1). All SP genotypes at these QTL peaks had positive effects except for the LG17 QTL in which SP had a negative effect on plate width (Fig. S10), similar to its negative effect on plate number (Fig. 3). Therefore, SP genotype at both LG19 and LG20 QTL peaks yielded the largest plate size and SP genotype at LG20 yielded the

largest plate height, whereas SP genotype at both LG19 and LG20 and SS genotype at LG17 yielded the largest plate width (Fig. S11).

The lasso regression approach produced genomic heritabilities higher than the summed PVEs in plate area (h^2 = 0.495; Sum_{PVE} = 0.276), plate height (h^2 = 0.501; Sum_{PVE} = 0.256), and plate width (h^2 = 0.317; Sum_{PVE} = 0.278; Table 1, Table S5), suggesting that additional unidentified loci may influence variation in these traits.

QTL mapping of body size

Females were significantly larger than males both in terms of standard length (SL; $x_{females}$ = 52.9 ± 0.57 [S.E.] mm; x_{males} = 49.0 ± 0.44 mm; $t_{190.36}$ = 5.33, $p < 0.05$) and body height (BH; $x_{females}$= 11.0 ± 0.15 mm; x_{males}= 10.4 ± 0.09 mm; $t_{174.57}$ = 3.28, $p < 0.05$). Two moderate-effect QTL at LG12 and LG16 influenced SL and a QTL on LG6 influenced BH (Table 1; Fig. 4). The lasso method estimated genomic heritabilities of h^2 = 0.263 for SL and h^2 = 0.206 for BH (Table S5), and the corresponding summed PVEs across QTL were Sum_{PVE} = 0.265 for SL and Sum_{PVE} = 0.107 for BH (Table 1). It is noteworthy that the peak on LG6 in the analysis of SL was close to significance (Fig. 4), indicating that this region might also affect standard length by affecting the body height.

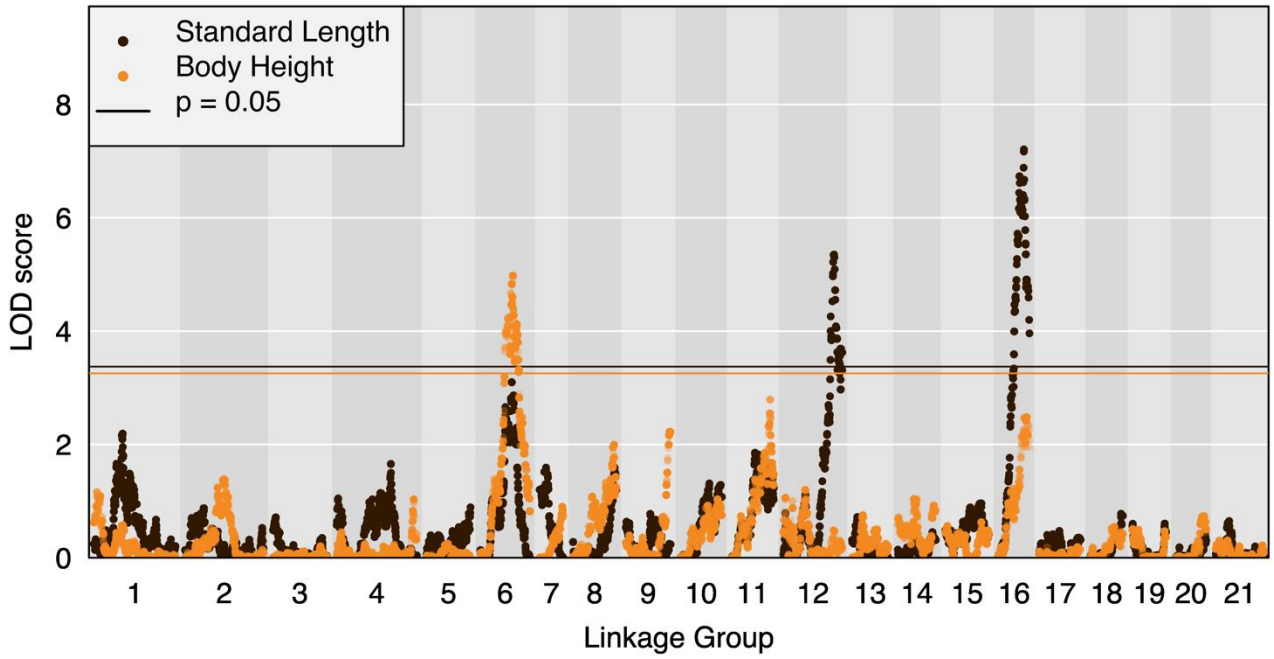

Figure 4. The QTL regions of body size variation. Horizontal lines show the significance threshold (p = 0.05) derived from 1000 permutation tests for each trait.

Candidate genes

All genes containing SNPs in identified QTL regions are listed in Table S3. For the plate number variation, we identified several candidate genes whose functions might be associated with stickleback skeletal development, including the *Eda* gene on LG4, the fibroblast growth factors on LG4 (*Fgf4*, *Fgf16*, *Fgf20*, Jovelin et al. 2007), the bone morphogenetic protein genes on LG17 (*Bmp7*, Shawi et al. 2008; *Bmp11*, Indjeian et al. 2016), and potentially the BMP-2-inducible protein kinase on LG13 (*Bmp2k*, Li and Cao 2006; Wang et al. 2020). For the plate size variation, the *fgf23* on LG19 and the *Bmp7* and *Bmp11* on LG17 were identified as candidate genes. The BMP family in particular has been suggested to control the height and width of armor plates in sticklebacks (Indjeian et al. 2016). In addition, the paired box proteins (*Pax6* on LG19 and *Pax7* on LG17) have been found associated with the development of vertebrae in lab mice (Lang et al. 2007) and thus might also be candidate genes controlling the armor plate development in sticklebacks. The *Fgf14* on LG16 was identified as a candidate gene controlling the body size development.

Discussion

Our study shows that variation in lateral plate number and plate size in the western European lineage (WL) of nine-spined sticklebacks were not fully controlled either by allelic variation in the same genetic loci as in the three-spined stickleback, or by the QTL controlling these phenotypes in the eastern European lineage (EL) of nine-spined sticklebacks. These results are consistent with the observation that pelvic armor morphology in the EL nine-spined sticklebacks is both more polygenic and heterogeneous (non-parallel) compared to the three-spined stickleback (Kemppainen et al. 2021). Hence, this study comprises yet another example of similar phenotypic changes being achieved by a variety of genetic architectures ranging from monogenic to oligo- or polygenic systems in the stickleback family Gasterosteidae (Colosimo et al. 2005; Shapiro et al. 2009; Yang et al. 2016; Kemppainen et al. 2021), rather than due to genetic parallelism governed by a few large-effect loci. Our findings highlight the notion that a diversity of genetic architectures can evolve to underpin similar phenotypic transitions, and that the frequency of reuse of the same genetic variation to achieve a given phenotypic transition (i.e., parallel evolution) seems to differ markedly between three- and nine-spined sticklebacks. Therefore, although freshwater populations of nine-spined sticklebacks are characterized by both small effective population sizes and low genetic connectivity (Shikano et al. 2010; Merilä 2014; Fang et al. 2021; Kivikoski et al. 2023), our results together with recent studies (Yang et al. 2016; Kemppainen et al. 2021) highlights that these two population demographic parameters alone do not necessarily limit evolutionary potential but rather result in a higher diversity of alleles underlying adaptive evolution.

Our results demonstrate that the genetic basis of lateral plate number variation in the WL nine-spined sticklebacks is controlled by at least three distinct moderate-effect QTL on different linkage groups, as well as unknown small-effect loci potentially across the genome as revealed by the lasso analyses. One of the moderate-effect QTL on LG4 contained the *Eda* gene known to be the major-

effect locus typically explaining ~69% to 98% variation in lateral plate numbers in three-spined sticklebacks (Table 2; Colosimo et al. 2004; Liu et al. 2014; Glazer et al. 2015; Erickson et al. 2016; Schluter et al. 2021). However, this moderate-effect QTL explained only ~9.9% of variation in lateral plate numbers in WL nine-spined sticklebacks. The two other QTL associated with lateral plate number variation in our study were located on LG13 and LG17 and they accounted for 18.6% and 11.0% of variation, respectively. Hence, collectively the three QTL identified in this study accounted for up to 39.6% of variation in lateral plate numbers. Nearly similar amount of variation (33%) in this trait was explained by four QTL in the EL nine-spined sticklebacks (Table 2; Yang et al. 2016), but none of the QTL controlling lateral plate numbers are shared between EL and WL fish. Therefore, the genetic architecture of lateral plate numbers is divergent not only between the genera *Gastoresteous* and *Pungitius* but also within the genus *Pungitius*.

Similar to the results regarding genetic architectures of later plate number variation, the three QTL controlling lateral plate size variation in WL nine-spined sticklebacks were different from those in three-spined sticklebacks (Table 2). These three QTL regions (on LG17, LG19, and LG20) accounted for up to 28% of variation in the lateral plate size. Because large effect sizes are more likely to be significant and detected as QTL regions, genetic loci of small effect sizes may not be detected due to lack of statistical power. In accordance with this, estimates from lasso regressions suggested that there are yet undetected small-effect loci (among the non-QTL SNPs) accounting for the unexplained variation (37% in plate area, 34% in plate height, and 20% in plate width, Table S5), indicating oligo- to polygenic inheritance of these traits. These results are consistent with the previous study showing that genetic architectures of pelvic reduction in nine-spined sticklebacks range from monogenic to oligogenic and polygenic inheritance (Kemppainen et al. 2021).

Among the moderate-effect QTL (on LG6, LG12, and LG16) explaining variation in standard length and body height of the WL nine-spined sticklebacks, only the LG12 QTL is shared with the QTL affecting body size in the EL nine-spined sticklebacks (on LG8, LG12, and LG13; Laine et al. 2013). Similar to the results regarding lateral plate variation, the body size variation also appears to

have different genetic architectures between EL and WL fishes. However, it is unclear whether the two LG12 QTL regions are actually the same or not in EL and WL, and it is hard to judge how different their genetic architectures are because our QTL analyses likely did not have power to detect loci of small effects. Nevertheless, genomic heritabilities for standard length and body depth (h^2 = 0.21 - 0.26) were very similar to the summed PVEs of individual QTL affecting these traits (0.11 - 0.27), suggesting an oligogenic basis of body size variation. This inference is supported by biometric estimates which have yielded very similar heritabilities within (h^2 = 0.13 - 0.18; Shimada et al. 2011) and among (h^2 = 0.07 - 0.25; Fraimout et al. 2022) population crosses in nine-spined sticklebacks.

We confirmed findings in Natri et al. (2019) that the ZW system inherited from *P. sinensis* controlled phenotypic sex of the hybrids between *P. sinensis* and *P. pungitius*. Our study also narrowed down the sex determination region of *P. sinensis* from around 19.4 cM in Natri et al. (2019) to two non-overlapping QTL regions of around total 1 cM on LG12 which explained 69% - 75% of the variation in sex. Recent studies found a translocated copy of the anti-Müllerian hormone gene (*Amh*) on the Y chromosome (*Amhy*) to be the candidate sex determination gene in several stickleback lineages (Jeffries et al. 2022), including the three-spined stickleback (Peichel et al. 2020), the blackspotted stickleback (*Gasterosteus wheatlandi*, Sardell et al. 2021), and the brook stickleback (*Culaea inconstans*, Jeffries et al. 2022), the latter being the sister genus of *Pungitius* (Guo et al. 2019). However, only the ancestral copy of the *Amh* gene is annotated in the nine-spined stickleback reference genome (on LG8; Varadharajan et al. 2019), indicating that it is unlikely the sex determination gene in *Pungitius* sticklebacks. In fact, so far no sex determination gene has been identified in any *Pungitius* sticklebacks despite known sex chromosomes (Jeffries et al. 2022). In this study, the SNPs mapped to sex-associated QTL regions fell into six annotated genes, among which the Ubiquitin carboxyl-terminal hydrolase 7 (*Usp7*) has been found to regulate sex chromosome development and interact with the sex determination region in mice (Luo et al. 2015; Dong et al. 2021). Therefore, *Usp7* is a candidate gene for sex determination of *P. sinensis*.

Among the genes that have been previously identified to have strong associations with the three-spined stickleback morphological development (summarized in Reid et al. 2021), only *Eda* on LG4 was included in our candidate gene list for the lateral plate number. Furthermore, we identified *Bmp2k* on LG13 as a candidate gene that impacts plate number variation in the nine-spined stickleback, and *Bmp7* on LG17 as a gene that potentially influences both plate number and plate width (although not plate area or height). Similarly, a recent study in the three-spined stickleback also found that the BMP pathway is a strong candidate mediating the effect of *Eda* on the development of lateral plates (Rodríguez-Ramírez et al. 2023). However, as all of the QTL regions in our study included tens to hundreds of genes, little confidence can be assigned to the identified candidate genes. Further narrowing of the QTL regions would require breeding individuals beyond F_2 generation, or adopting genome-wide association approaches with larger sample sizes than what was available for this study.

The strong isolation by distance in the sea and severe bottlenecks associated with freshwater colonisations have led to the prediction that nine-spined sticklebacks are more limited in reaching their phenotypic optima when colonising freshwater habitats compared to three spined sticklebacks (Fang et al. 2021). This prediction was supported by the observation that in three freshwater (pond) populations of EL nine-spined sticklebacks, pelvic reduction was only complete in one population where it was controlled by a single large-effect locus (*pitx*1), whereas the other two populations only showed some level of pelvic reduction possibly controlled by alternative medium- or small-effect alleles at other QTL regions (Kemppainen et al. 2021). Similarly, here we showed that the reduction of lateral plate numbers in freshwater WL nine-spined sticklebacks is controlled by multiple medium- to small-effect loci that are different from those in EL nine-spined sticklebacks and the large-effect *Eda* gene in three-spined sticklebacks. Accordingly, empirical evidence rejected the hypothesis of parallel evolution in the repeatable phenotypic changes of freshwater *Pungitius* sticklebacks, but indicated non-parallel and possibly redundant genetic architectures leading to similar phenotypic changes. Such redundancy is likely crucial for the evolutionary potential of

474 species and populations facing rapid environmental changes, especially in fragmented habitats
475 causing increased genetic differentiation and bottlenecks. For the species with fragmented small
476 populations, redundant genetic architectures increase the likelihood that at least some populations
477 can adapt to some novel environmental pressures, but it is difficult to achieve adaptation in all traits
478 within one population, and the long term species survival probability will still depend on the spread
479 of adaptive alleles across populations via gene flow.

480

481 **Conclusions and outlook**

482 In conclusion, our results add to the growing evidence (Shapiro et al. 2009; Shikano et al. 2013;
483 Yang et al. 2016; Fang et al. 2020; Kemppainen et al. 2021) that the repeatability of evolutionary
484 transitions in response to similar selection pressures in *Pungitius* sticklebacks is often underlied by
485 different genetic architectures of moderate- to small-effect loci. This is in stark contrast to the
486 situation in the closely related three-spined stickleback which tends to utilize the same major-effect
487 loci in independent colonizations of freshwater habitats. However, even in the case of the three-
488 spined stickleback, growing evidence suggests that genetic parallelism in adaptation to freshwater is
489 not as prevalent as early studies conducted in the Eastern Pacific region suggested: a greatly
490 reduced degree of genetic parallelism has been found in the Atlantic basin likely due to variation
491 lost during colonizations as well as reduced gene flow among these populations (DeFaveri et al.
492 2011; Fang et al. 2020; Dahms et al. 2022). The same also applies to stream-lake populations of
493 three-spined sticklebacks experiencing reduced gene flow (Conte et al., 2012; Conte et al., 2015;
494 Stuart et al., 2017; reviewed in Kemppainen et al. 2021). We suggest that further focus on genetic
495 underpinnings of phenotypic variation in the morphologically and genetically diverse stickleback
496 genus *Pungitius* (Guo et al. 2019) can provide a useful framework to quantify how the likelihood of
497 genetic parallelism underlying similar phenotypic changes decreases with increasing evolutionary

498 distance between taxa (Elmer and Meyer 2011; Conte *et al.* 2012) and also inform us about

499 variation in species' responses to changing environments (Bay et al. 2017).

500

501 **Tables**

502 **Table 1. The QTL peaks for phenotypic traits.** LG = linkage group, cM = centimorgan, PVE =
503 percentage of variation explained.

Phenotype	LG	Peak (cM)	95%CI low (cM)	95%CI high (cM)	Range (cM)	LOD	PVE (%)	NO. SNPs in 95% CI
Sex	12	11.286	10.819	11.286	0.467	61.08	74.98	18
Sex	12	13.623	13.623	14.090	0.467	51.25	68.74	25
Standard Length	12	87.896†	81.591	92.927	11.336	5.35	11.43	139
Standard Length	16	43.088	32.301	45.438	13.137	7.21	15.08	110
Body Height	6	55.305	42.172	63.721	21.549	4.98	10.68	547
Plate number	4	137.699	133.021	137.699	4.678	4.58	9.87	1531
Plate number	13	64.174	60.436	65.109	4.673	9.09	18.64	428
Plate number	17	62.363	47.838	70.352	22.514	5.16	11.04	2677
Plateness	13	63.240	56.693	65.109	8.416	4.92	10.57	494
Plate Area	19	36.939‡	30.427	58.042	27.615	3.68	8.01	2512
Plate Area	20	53.440	48.767	53.440	4.673	9.63	19.63	1642
Plate Height	20	53.440	49.234	53.440	4.206	13.02	25.58	1626
Plate Width	17	65.635	48.772	70.352	21.580	3.84	8.33	2663
Plate Width	19	33.707	4.677	56.172	51.495	3.26	7.12	2688
Plate Width	20	53.440	50.169	53.440	3.271	5.81	12.35	1597

504 † Pseudomarker (the nearest non-pseudo genetic position at 88.191).
505 ‡ Pseudomarker (the nearest non-pseudo genetic position at 36.043).
506

Table 2. Comparison of the genetic architecture underlying the variation of lateral plate number and size in stickleback fishes. Populations used in the cross experiments are given in parentheses. EL = eastern European lineage, WL = western European lineage.

Species	Lateral plate number		Lateral plate size		Reference
	QTL	PVE (%)	QTL	PVE (%)	
Gasterosteus aculeatus (Japan × Canada)	LG4 LG7 LG10 LG26†	76.9 3.7 6.5 4.5	LG4 LG7 LG25†	11.5 - 12.9 10.3 - 11.1 17.9 - 28.9	Colosimo et al. 2004
Gasterosteus aculeatus (Finland)	LG4 LG9 LG21	74.4 9.1 10.6	-	-	Liu et al. 2014
Gasterosteus aculeatus (Canada × US)	LG4 LG7	95.7 - 97.8 13.3‡	-	-	Glazer et al. 2015
Gasterosteus aculeatus (Canada)	LG1 LG3 LG4 LG5 LG7 LG21	1.5 - 1.6 2.4 68.8 - 75.8 4.5 2.9 - 4.2 1.6 - 7.5	-	-	Erickson et al. 2016
Gasterosteus aculeatus (Canada)	LG4	85.8	-	-	Schluter et al. 2021
Pungitius pungitius (Canada × Alaska)	LG12§	28.4 - 30.1	-	-	Shapiro et al. 2009
Pungitius pungitius (Finland EL)	LG8 LG12 LG20 LG21	8.7 7.3 8.0 - 11.3 8.6 - 10.0	-	-	Yang et al. 2016
Pungitius pungitius (Japan *P. sinensis* × Belgium WL)	LG4 LG13 LG17	9.9 18.6 11.0	LG17 LG19 LG20	8.3 7.1 - 8.0 12.4 - 25.6	This study

† The original linkage group studies in *Gasterosteus aculeatus* were based on a linkage map with 26 LGs before consolidation to the 21 confirmed chromosomes.

‡ Residual variance in *Eda* heterozygotes

§ The same region control sex

References

Bailey, S. F., Blanquart, F., Bataillon, T., & Kassen, R. (2017). What drives parallel evolution? How population size and mutational variation contribute to repeated evolution. *BioEssays*, *39*(1), 1-9.

Banarescu, P.M. and Paepke, H.J. (2001). The freshwater fishes of Europe, vol 5/III. *AULA, Wiebelsheim*.

Bay, R. A., Rose, N., Barrett, R., Bernatchez, L., Ghalambor, C. K., Lasky, J. R., ... & Ralph, P. (2017). Predicting responses to contemporary environmental change using evolutionary response architectures. *American Naturalist*, *189*(5), 463-473.

Bernatchez, L., Renaut, S., Whiteley, A. R., Derome, N., Jeukens, J., Landry, L., ... & St-Cyr, J. (2010). On the origin of species: insights from the ecological genomics of lake whitefish. *Philosophical Transactions of the Royal Society B: Biological Sciences*, *365*(1547), 1783-1800.

Bolnick, D. I., Barrett, R. D., Oke, K. B., Rennison, D. J., & Stuart, Y. E. (2018). (Non) parallel evolution. *Annual Review of Ecology, Evolution, and Systematics*, *49*, 303-330.

Broman, K. W., & Sen, S. (2009). *A Guide to QTL Mapping with R/qtl* (Vol. 46). New York: Springer.

Broman, K. W., Gatti, D. M., Simecek, P., Furlotte, N. A., Prins, P., Sen, Ś., ... & Churchill, G. A. (2019). R/qtl2: software for mapping quantitative trait loci with high-dimensional data and multiparent populations. *Genetics*, *211*(2), 495-502.

Chan, Y. F., Marks, M. E., Jones, F. C., Villarreal, G., Shapiro, M. D., Brady, S. D., Southwick, A. M., Absher, D. M., Grimwood, J., Schmutz, J., Myers, R. M., Petrov, D., Jónsson, B., Schluter, D., Bell, M. A., & Kingsley, D. M. (2010). Adaptive evolution of pelvic reduction in sticklebacks by recurrent deletion of a pitxl enhancer. *Science*, *327*(5963), 302–305. https://doi.org/10.1126/SCIENCE.1182213/

Colosimo, P. F., Peichel, C. L., Nereng, K., Blackman, B. K., Shapiro, M. D., Schluter, D., & Kingsley, D. M. (2004). The genetic architecture of parallel armor plate reduction in threespine sticklebacks. *PLoS Biology*, 2(5), e109.

Colosimo, P. F., Hosemann, K. E., Balabhadra, S., Villarreal, G., Dickson, H., Grimwood, J., Schmutz, J., Myers, R. M., Schluter, D., & Kingsley, D. M. (2005). Widespread parallel evolution in sticklebacks by repeated fixation of ectodysplasin alleles. *Science*, *307*(5717), 1928–1933. https://doi.org/10.1126/SCIENCE.1107239

Conte G. L., Arnegard M. E., Peichel C. L., Schluter D. (2012). The probability of genetic parallelism and convergence in natural populations. *Proc. Biol. Sci.*, 279, 5039–5047

Conte, G. L., Arnegard, M. E., Best, J., Chan, Y. F., Jones, F. C., Kingsley, D. M., ... & Peichel, C. L. (2015). Extent of QTL reuse during repeated phenotypic divergence of sympatric threespine stickleback. *Genetics*, *201*(3), 1189-1200.

Coyle, S. M., Huntingford, F. A., & Peichel, C. L. (2007). Parallel evolution of Pitx1 underlies pelvic reduction in Scottish threespine stickleback (*Gasterosteus aculeatus*). Journal of Heredity, 98(6), 581-586.

555 Dahms, C., Kemppainen, P., Zanella, L. N., Zanella, D., Carosi, A., Merilä, J., & Momigliano, P.
556 (2022). Cast away in the Adriatic: Low degree of parallel genetic differentiation in three-spined
557 sticklebacks. *Molecular Ecology*, *31*(4), 1234-1253.

558 Danecek, P., Bonfield, J. K., Liddle, J., Marshall, J., Ohan, V., Pollard, M. O., ... & Li, H. (2021).
559 Twelve years of SAMtools and BCFtools. *Gigascience*, *10*(2), giab008.

560 DeFaveri, J., Shikano, T., Shimada, Y., Goto, A., & Merilä, J. (2011). Global analysis of genes
561 involved in freshwater adaptation in threespine sticklebacks (*Gasterosteus aculeatus*). *Evolution*,
562 *65*(6), 1800-1807.

563 DeFaveri, J., Jonsson, P. R., & Merilä, J. (2013). Heterogeneous genomic differentiation in marine
564 threespine sticklebacks: adaptation along an environmental gradient. *Evolution*, *67*(9), 2530-2546.

565 Dong, X., Xu, X., Yang, C., Luo, Y., Wu, Y., & Wang, J. (2021). USP7 regulates the proliferation
566 and differentiation of ATDC5 cells through the Sox9-PTHrP-PTH1R axis. *Bone*, *143*, 115714.

567 Elmer, K. R., Kusche, H., Lehtonen, T. K., & Meyer, A. (2010). Local variation and parallel
568 evolution: morphological and genetic diversity across a species complex of neotropical crater lake
569 cichlid fishes. *Philosophical Transactions of the Royal Society B: Biological Sciences*, *365*(1547),
570 1763-1782.

571 Elmer, K.R. & Meyer, A. (2011). Adaptation in the age of ecological genomics: insights from
572 parallelism and convergence. *Trends in Ecology & Evolution*, *26*(6), 298-306.

573 Erickson, P. A., Glazer, A. M., Killingbeck, E. E., Agoglia, R. M., Baek, J., Carsanaro, S. M., ... &
574 Miller, C. T. (2016). Partially repeatable genetic basis of benthic adaptation in threespine
575 sticklebacks. *Evolution*, *70*(4), 887-902.

576 Fang, B., Kemppainen, P., Momigliano, P., Feng, X., & Merilä, J. (2020). On the causes of
577 geographically heterogeneous parallel evolution in sticklebacks. *Nature Ecology & Evolution*, *4*(8),
578 1105-1115.

579 Fang, B., Kemppainen, P., Momigliano, P., & Merilä, J. (2021). Population structure limits parallel
580 evolution in sticklebacks. *Molecular Biology and Evolution*, *38*(10), 4205–4221.
581 https://doi.org/10.1093/

582 Feng, X., Merilä, J., & Löytynoja, A. (2022). Complex population history affects admixture
583 analyses in nine-spined sticklebacks. Molecular Ecology, 31(20), 5386-5401.

584 Fraimout, A., Li, Z., Sillanpää, M.J. & Merilä, J. (2022). Age-dependent genetic architecture across
585 ontogeny of body size in sticklebacks. *Proceedings of the Royal Society B*, *289*(1975), 20220352.

586 Glazer, A. M., Killingbeck, E. E., Mitros, T., Rokhsar, D. S., & Miller, C. T. (2015). Genome
587 assembly improvement and mapping convergently evolved skeletal traits in sticklebacks with
588 genotyping-by-sequencing. *G3: Genes, Genomes, Genetics*, *5*(7), 1463-1472.

589 Guo, B., Fang, B., Shikano, T., Momigliano, P., Wang, C., Kravchenko, A., & Merilä, J. (2019). A
590 phylogenomic perspective on diversity, hybridization and evolutionary affinities in the stickleback
591 genus Pungitius. *Molecular Ecology*, *28*(17), 4046-4064.

592 Herczeg, G., Turtiainen, M., & Merilä, J. (2010). Morphological divergence of North-European
593 nine-spined sticklebacks (*Pungitius pungitius*): signatures of parallel evolution. *Biological Journal*
594 *of the Linnean Society*, 101(2), 403-416.

595 Indjeian, V. B., Kingman, G. A., Jones, F. C., Guenther, C. A., Grimwood, J., Schmutz, J., ... &
596 Kingsley, D. M. (2016). Evolving new skeletal traits by cis-regulatory changes in bone
597 morphogenetic proteins. *Cell*, 164(1-2), 45-56.

598 Jeffries, D. L., Mee, J. A., & Peichel, C. L. (2022). Identification of a candidate sex determination
599 gene in Culaea inconstans suggests convergent recruitment of an Amh duplicate in two lineages of
600 stickleback. *Journal of evolutionary biology*, *35*(12), 1683-1695.

601 Jones, F. C., Grabherr, M. G., Chan, Y. F., Russell, P., Mauceli, E., Johnson, J., ... & Kingsley, D.
602 M. (2012). The genomic basis of adaptive evolution in threespine sticklebacks. Nature, 484(7392),
603 55-61.

604 Jovelin R., He X.J.,Amores A., Yan Y.L., Shi R.H.,Qin B.F., Roe B. Cresko W.A., &Postlethwait
605 J.H. (2007). Duplication and divergence of fgf8 functions in teleost development and evolution.
606 *Journal of Experimental Zoology Part B: Molecular and Developmental Evolution* 308(6): 730-
607 743.

608 Kemppainen, P., Li, Z., Rastas, P., Löytynoja, A., Fang, B., Yang, J., ... & Merilä, J. (2021).
609 Genetic population structure constrains local adaptation in sticklebacks. *Molecular Ecology*, *30*(9),
610 1946-1961.

611 Kivikoski, M., Rastas, P., Löytynoja, A., & Merilä, J. (2021). Automated improvement of
612 stickleback reference genome assemblies with Lep-Anchor software. *Molecular Ecology*
613 *Resources*, *21*(6), 2166-2176.

614 Kivikoski, M., Rastas, P., Löytynoja, A., & Merilä, J. (2023). Predicting recombination frequency
615 from map distance. *Heredity*, *130*(3), 114-121.

616 Laine, V. N., Shikano, T., Herczeg, G., Vilkki, J., & Merilä, J. (2013). Quantitative trait loci for
617 growth and body size in the nine-spined stickleback *Pungitius pungitius* L. *Molecular Ecology*,
618 *22*(23), 5861–5876. https://doi.org/10.1111/MEC.12526

619 Lang, D., Powell, S. K., Plummer, R. S., Young, K. P., & Ruggeri, B. A. (2007). PAX genes: roles
620 in development, pathophysiology, and cancer. *Biochemical pharmacology*, 73(1), 1-14.

621 Lee, K., & Coop, G. (2017). Distinguishing among modes of convergent adaptation using
622 population genomic data. *Genetics*, *207*, 1591– 1619. https://doi.org/10.1534/genetics.117.300417

623 Leinonen, T., McCairns, R. S., Herczeg, G., & Merilä, J. (2012). Multiple evolutionary pathways to
624 decreased lateral plate coverage in freshwater threespine sticklebacks. Evolution, 66(12), 3866-
625 3875.

626 Li, H., & Durbin, R. (2009). Fast and accurate short read alignment with Burrows–Wheeler
627 transform. *Bioinformatics*, *25*(14), 1754-1760.

628 Li, H. (2011). A statistical framework for SNP calling, mutation discovery, association mapping
629 and population genetical parameter estimation from sequencing data. *Bioinformatics*, *27*(21), 2987-
630 2993.

631 Li, X., & Cao, X. U. (2006). BMP signaling and skeletogenesis. *Annals of the New York Academy*
632 *of Sciences*, 1068(1), 26-40.

Li, Z., Guo, B., Yang, J., Herczeg, G., Gonda, A., Balázs, G., ... & Merilä, J. (2017). Deciphering the genomic architecture of the stickleback brain with a novel multilocus gene-mapping approach. *Molecular Ecology*, *26*(6), 1557-1575.

Li, Z., Kemppainen, P., Rastas, P., & Merilä, J. (2018). Linkage disequilibrium clustering-based approach for association mapping with tightly linked genomewide data. *Molecular Ecology Resources*, *18*(4), 809-824.

Liu, J., Shikano, T., Leinonen, T., Cano, J. M., Li, M. H., & Merilä, J. (2014). Identification of major and minor QTL for ecologically important morphological traits in three-spined sticklebacks (*Gasterosteus aculeatus*). *G3: Genes, Genomes, Genetics*, *4*(4), 595-604.

Loehr, J., Leinonen, T., Herczeg, G., O'Hara, R. B., & Merilä, J. (2012). Heritability of asymmetry and lateral plate number in the threespine stickleback. PLoS One, 7(7), e39843.

Luo, M., Zhou, J., Leu, N. A., Abreu, C. M., Wang, J., Anguera, M. C., ... & Wang, P. J. (2015). Polycomb protein SCML2 associates with USP7 and counteracts histone H2A ubiquitination in the XY chromatin during male meiosis. *PLoS Genetics*, *11*(1), e1004954.

MacPherson, A., & Nuismer, S. L. (2017). The probability of parallel genetic evolution from standing genetic variation. *Journal of Evolutionary Biology*, *30*(2), 326-337.

Marchinko, K. B., & Schluter, D. (2007). Parallel evolution by correlated response: lateral plate reduction in threespine stickleback. Evolution, 61(5), 1084-1090.

Martin, A., & Orgogozo, V. (2013). The loci of repeated evolution: a catalog of genetic hotspots of phenotypic variation. Evolution, 67(5), 1235-1250.

Merilä, J. (2013). Nine-spined stickleback (*Pungitius pungitius*): an emerging model for evolutionary biology research. *Annals of the New York Academy of Sciences*, *1289*(1), 18-35.

Merilä, J. (2014). Lakes and ponds as model systems to study parallel evolution. *Journal of Limnology*. 73:33–45.

Miller, M. R., Dunham, J. P., Amores, A., Cresko, W. A. and Johnson, E. A. (2007). Rapid and cost-effective polymorphism identification and genotyping using restriction site associated DNA (RAD) markers. *Genome research*, 17, 240–248.

Miller, C. T., Glazer, A. M., Summers, B. R., Blackman, B. K., Norman, A. R., Shapiro, M. D., Cole, B. L., Peichel, C. L., Schluter, D., & Kingsley, D. M. (2014). Modular skeletal evolution in sticklebacks is controlled by additive and clustered quantitative trait loci. *Genetics*, *197*(1), 405–420. https://doi.org/10.1534/GENETICS.114.162420

Natri, H. M., Merilä, J., & Shikano, T. (2019). The evolution of sex determination associated with a chromosomal inversion. *Nature Communications*, *10*(1), 1-13.

O'Brown, N. M., Summers, B. R., Jones, F. C., Brady, S. D., & Kingsley, D. M. (2015). A recurrent regulatory change underlying altered expression and Wnt response of the stickleback armor plates gene EDA. *elife*, *4*, e05290.

Peichel, C. L., & Marques, D. A. (2017). The genetic and molecular architecture of phenotypic diversity in sticklebacks. Philosophical Transactions of the Royal Society B: Biological Sciences, 372(1713), 20150486.

672 Peichel, C. L., McCann, S. R., Ross, J. A., Naftaly, A. F., Urton, J. R., Cech, J. N., ... & White, M.
673 A. (2020). Assembly of the threespine stickleback Y chromosome reveals convergent signatures of
674 sex chromosome evolution. Genome Biology, 21(1), 1-31.

675 Ralph, P. L., & Coop, G. (2015). The role of standing variation in geographic convergent
676 adaptation. *American Naturalist*, *186*(S1), S5-S23.

677 R Core Team (2022). R: A language and environment for statistical computing. R Foundation for
678 Statistical Computing, Vienna, Austria. https://www.R-project.org/.

679 Rastas, P. (2017). Lep-MAP3: robust linkage mapping even for low-coverage whole genome
680 sequencing data. *Bioinformatics*, *33*(23), 3726-3732.

681 Rastas, P. (2020). Lep-Anchor: automated construction of linkage map anchored haploid genomes.
682 *Bioinformatics*, *36*(8), 2359-2364.

683 Reid, K., Bell, M. A., & Veeramah, K. R. (2021). Threespine stickleback: A model system for
684 evolutionary genomics. *Annual review of genomics and human genetics*, *22*, 357-383.
685 https://doi.org/10.1146/annurev-genom-111720

686 Roberts Kingman, G. A., Vyas, D. N., Jones, F. C., Brady, S. D., Chen, H. I., Reid, K., ... &
687 Veeramah, K. R. (2021). Predicting future from past: The genomic basis of recurrent and rapid
688 stickleback evolution. *Science Advances*, *7*(25), eabg5285.

689 Rodríguez-Ramírez, C. E., Hiltbrunner, M., Saladin, V., Walker, S., Urrutia, A., & Peichel, C. L.
690 (2023). Molecular mechanisms of *Eda*-mediated adaptation to freshwater in threespine stickleback.
691 *Molecular Ecology*, 00, 1– 19. https://doi.org/10.1111/mec.16989

692 Sardell, J. M., Josephson, M. P., Dalziel, A. C., Peichel, C. L., & Kirkpatrick, M. (2021).
693 Heterogeneous histories of recombination suppression on stickleback sex chromosomes. *Molecular*
694 *Biology and Evolution*, *38*(10), 4403-4418.

695 Schlötterer, C. (2023). How predictable is adaptation from standing genetic variation? Experimental
696 evolution in Drosophila highlights the central role of redundancy and linkage disequilibrium.
697 *Philosophical Transactions of the Royal Society B*, *378*(1877), 20220046.

698 Schluter, D., Clifford, E. A., Nemethy, M., & McKinnon, J. S. (2004). Parallel evolution and
699 inheritance of quantitative traits. *American Naturalist*, *163*(6), 809-822.

700 Schluter, D., Marchinko, K. B., Arnegard, M. E., Zhang, H., Brady, S. D., Jones, F. C., Bell, M. A.,
701 & Kingsley, D. M. (2021). Fitness maps to a large-effect locus in introduced stickleback
702 populations. *Proceedings of the National Academy of Sciences of the United States of America*,
703 *118*(3), e1914889118. https://doi.org/10.1073/PNAS.1914889118

704 Shapiro, M. D., Summers, B. R., Balabhadra, S., Aldenhoven, J. T., Miller, A. L., Cunningham, C.
705 B., ... & Kingsley, D. M. (2009). The genetic architecture of skeletal convergence and sex
706 determination in ninespine sticklebacks. Current Biology, 19(13), 1140-1145.

707 Shawi, M., & Serluca, F. C. (2008). Identification of a *BMP7* homolog in zebrafish expressed in
708 developing organ systems. *Gene Expression Patterns*, 8(6), 369-375.

709 Shikano, T., Shimada, Y., Herczeg, G., & Merilä, J. (2010). History vs. habitat type: explaining the
710 genetic structure of European nine-spined stickleback (*Pungitius pungitius*) populations. *Molecular*
711 *Ecology*, *19*(6), 1147-1161.

712 Shikano, T., Laine, V. N., Herczeg, G., Vilkki, J., & Merilä, J. (2013). Genetic architecture of
713 parallel pelvic reduction in ninespine sticklebacks. *G3: Genes, Genomes, Genetics*, *3*(10), 1833-
714 1842.

715 Shimada, Y., Shikano, T., Kuparinen, A., Gonda, A., Leinonen, T. & Merilä, J. (2011). Quantitative
716 genetics of body size and timing of maturation in two nine-spined stickleback (*Pungitius pungitius*)
717 populations. *PLoS One*, *6*(12), e28859.

718 Smith, S. R., Amish, S. J., Bernatchez, L., Le Luyer, J., C. Wilson, C., Boeberitz, O., ... & Scribner,
719 K. T. (2020). Mapping of adaptive traits enabled by a high-density linkage map for Lake Trout. *G3:*
720 *Genes, Genomes, Genetics*, *10*(6), 1929-1947.

721 Stewart, J. R., & Thompson, M. B. (2009). Parallel evolution of placentation in Australian scincid
722 lizards. *Journal of Experimental Zoology Part B: Molecular and Developmental Evolution*, *312*(6),
723 590-602.

724 Stuart, Y. E., Veen, T., Weber, J. N., Hanson, D., Ravinet, M., Lohman, B. K., ... & Bolnick, D. I.
725 (2017). Contrasting effects of environment and genetics generate a continuum of parallel evolution.
726 *Nature Ecology & Evolution*, *1*(6), 0158.

727 Teacher, A. G., Shikano, T., Karjalainen, M. E., & Merilä, J. (2011). Phylogeography and genetic
728 structuring of European nine-spined sticklebacks (Pungitius pungitius)—mitochondrial DNA
729 evidence. *PLoS One*, *6*(5), e19476.

730 Thompson, K. A., Osmond, M. M., & Schluter, D. (2019). Parallel genetic evolution and speciation
731 from standing variation. *Evolution Letters*, *3*, 129– 141. https://doi.org/10.1002/evl3.106

732 Trokovic, N., Herczeg, G., Scott McCairns, R. J., Izza Ab Ghani, N., & Merilä, J. (2011).
733 Intraspecific divergence in the lateral line system in the nine-spined stickleback (Pungitius
734 pungitius). *Journal of Evolutionary Biology*, 24, 1546-1558.

735 Varadharajan, S., Rastas, P., Löytynoja, A., Matschiner, M., Calboli, F. C., Guo, B., ... & Merilä, J.
736 (2019). A high-quality assembly of the nine-spined stickleback (*Pungitius pungitius*)
737 genome. *Genome Biology and Evolution*, *11*(11), 3291-3308.

738 Wang, M., Zhang, T., Zhang, X., Jiang, Z., Peng, M., & Huang, Z. (2020). *BMP2K* dysregulation
739 promotes abnormal megakaryopoiesis in acute megakaryoblastic leukemia. *Cell & Bioscience*, 10,
740 1-14.

741 Yang, J., Guo, B., Shikano, T., Liu, X., & Merilä, J. (2016). Quantitative trait locus analysis of
742 body shape divergence in nine-spined sticklebacks based on high-density SNP-panel. *Scientific*
743 *Reports*, *6*(1), 1-16.

744